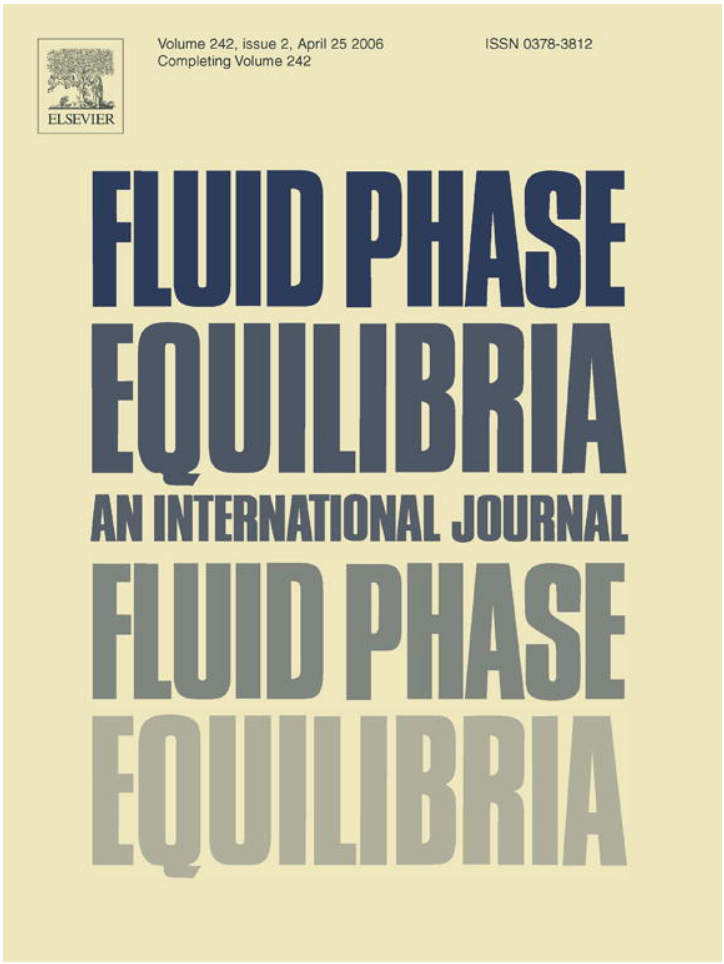

Available online at www.sciencedirect.com
SCIENCE DIRECT
Fluid Phase Equilibria 242 (2006) 210–219
FLUID PHASE EQUILIBRIA
www.elsevier.com/locate/fluid

Liquid–liquid equilibrium of (perfluoroalkane + alkane) binary mixtures

Maria J. Pratas de Melo [a], Ana M.A. Dias [a], Marijana Blesic [b], Luís P.N. Rebelo [b], Lourdes F. Vega [c], João A.P. Coutinho [a], Isabel M. Marrucho [a,*]

[a] *CICECO, Universidade de Aveiro, 3810-193 Aveiro, Portugal*
[b] *Instituto de Tecnologia Química e Biológica, ITQB2, Universidade Nova de Lisboa, Av. República, Apartado 127, 2780-901 Oeiras, Portugal*
[c] *Institut de Ciència de Materials de Barcelona, Consejo Superior de Investigaciones Científicas (ICMAB-CSIC), Campus de la U.A.B., 08193 Bellaterra, Barcelona, Spain*

Received 1 February 2006; accepted 2 February 2006

Abstract

Despite the structural similarity between perfluoroalkanes (PFCs) and alkanes (HCs), mixtures containing these two classes of compounds present large deviations from Raoult's law and extended immiscibility regions. The study of these mixtures is of great interest for both practical applications and testing or improving theories of mixtures as well as for the general understanding of solute–solvent interactions. In this work, new liquid–liquid equilibrium (LLE) data for mixtures of perfluoro-*n*-octane and linear alkanes from C_6 to C_9 are presented. Data were measured at atmospheric pressure by turbidimetry and at pressures up to 150 MPa using a laser light scattering technique. The binary liquid–liquid equilibrium data were correlated using relations derived from renormalization group (RG) theory and the Modified UNIFAC with temperature dependent interaction parameters. The soft-SAFT equation of state (EoS) was also used, with parameters taken from vapour–liquid equilibrium (VLE) data to study their transferability to liquid–liquid equilibrium data. It is shown that using those parameters soft-SAFT can provide a good description of the data measured far from the critical point at atmospheric pressure and a correct dependence of the critical temperature up to 150 MPa if the size interaction parameter is also considered.

Keywords: Perfluoro-*n*-octane; Linear alkanes; Liquid–liquid equilibrium; Soft-SAFT EoS; Renormalization group theory; Modified UNIFAC

1. Introduction

The mutual incompatibility between perfluoroalkanes (PFCs) and alkanes (HCs) generates a set of interesting phenomena in all states of matter expressed as large regions of liquid–liquid immiscibility, large positive deviations from Raoult's law, and large positive excess properties [1,2]; microphase separation, segregation, and self-assembly [3], negative aneotropy or minima in the surface tension versus composition diagrams [4], among others are also found. All these phenomena reflect the bulk thermodynamics of these mixtures, which are characterized by weak, unlike interactions.

Since the late 1940s, the potential application of these systems as refrigerant mixtures or as immiscible solvents has motivated their study. The hydrophobicity of fluorinated compounds (that makes them immiscible at room temperature with water and with many common organic solvents) as well as their ability to form a homogenous solution at elevated temperatures with several of these solvents together with their inertness, their solubility in supercritical CO_2, and their ability to dissolve gases, assemble them and their mixtures interesting materials to be used in new applications. These include their use as two-phase reaction media in a novel technique known as "*Fluorous Phase Organic Synthesis*" (FPOS) [5–7].

A bibliographic review on available experimental data of (PFC + HC) systems is compiled in Table 1. It summarizes the methods and experimental conditions used to perform liquid–liquid solubility measurements for mixtures of linear,

* Corresponding author. Tel.: +351 234 370200; fax: +351 234 380074.
E-mail address: imarrucho@dq.ua.pt (I.M. Marrucho).

0378-3812/$ – see front matter © 2006 Elsevier B.V. All rights reserved.
doi:10.1016/j.fluid.2006.02.003

Table 1
Compilation of references reporting experimental liquid–liquid solubility data for perfluoroalkane + alkane systems

System	Method	T range (K)	P range (MPa)	Reference
$C_7F_{14} + C_6H_6$	Synthetic	308–359	0.1	Hildebrand and Cochran [8]
$C_7F_{14} + C_7H_8$		316–362		
$C_7F_{16} + C_6H_6$	Synthetic	330–387	0.1	Hildebrand et al. [9]
$C_7F_{16} + C_7H_{16}$		300–323		
$C_5F_{12} + C_5H_{12}$	Synthetic		0.1	Simons and Dunlap [10]
$C_4F_{10} + C_4H_{10}$	Synthetic		0.1	Simons and Mausteller [11]
$C_7F_{16} + C_8H_{18}$	Synthetic	300–341	0.1	Campbell and Hickman [12]
$C_7F_{16} + C_6H_{14}$	Synthetic	283–302	0.1	Hickman [13]
$C_6F_{14} + C_6H_{14}$	Synthetic	250–294	0.1	Bedford and Dunlap [14]
$C_6F_{14} + C_6H_{14}$	Synthetic	290–295	0.1	Lepori et al. [1]
$C_6F_{14} + C_7H_{16}$		300–315		
$C_6F_{14} + C_8H_{18}$		286–325		
$C_8F_{18} + C_6H_{14}$	Synthetic	260–314	0.1	Lo Nostro et al. [3]
$C_8F_{18} + C_7H_{16}$		293–331		
$C_8F_{18} + C_8H_{18}$		295–349		

cyclic and aromatic alkanes with perfluoroalkanes that are liquid at ambient temperature. Although significant experimental data have been reported, the fact is that, to date, there are aspects related to these mixtures that are not yet completely understood. As a consequence, there is no single method/model able to correctly predict or describe this type of mixtures.

In the early 1950s, it was believed that (PFC + HC) mixtures would be completely miscible in all proportions and that the regular solution theory [15] would describe these mixtures, at least qualitatively. When the first results for LLE data begun to be published – revealing their high non-ideality – new explanations had to be considered to account for their anomalous behaviour. Several approaches or proposals to solve this issue were presented. For instance, the failure of the geometric combining rule due to the interpenetration between neighboring C–H groups which leads to an abnormally strong hydrocarbon–hydrocarbon interaction energy, were corrected by an empirical shift in the solubility parameter, δ, of the hydrocarbons. Additionally, corrections to the regular solution theory to include the effect of volume changes that occur on mixing and modifications of regular solution theory to take into account size and ionization potential differences between the two components were considered. However, as reported by Scott [16] none of the suggestions fully accounted for the anomalous behaviour of all systems investigated. In the 1970s, Siebert and Knobler [17] measured the second virial coefficients of *n*-alkanes, perfluoro-*n*-alkanes, and their mixtures and concluded that the anomalous behaviour of alkane + perfluoroalkane systems was due to the failure of the geometric-mean rule to describe the unusually weak hydrocarbon–fluorocarbon attractive interaction. They discussed possible reasons for such a weak, unlike interaction between the two components: non-central forces, large ionization potential differences, and large size differences, concluding that the observed deviation from the geometric-mean prediction was most likely due to the latter. This explanation had previously been suggested by Dyke et al. [18] and Rowlinson [19] from studies of the gas–liquid critical line and a review of the data available, respectively. The results indicated that the interactions between perfluoroalkanes and alkanes were about 10% weaker than the geometric mean of the like-molecule interactions.

Similar conclusions were drawn by Mousa et al. [20] when they tried to apply the theory of conformal solutions to calculate the critical properties of several perfluoralkane + alkane mixtures. The authors observed that accurate results were obtained only when an unlike parameter equal to 0.92 was used to calculate the mixed interaction constant. Archer et al. [21] reported the first attempt to account for the liquid–liquid thermodynamics of alkane + perfluoroalkanes mixtures using the bonded hard-sphere (BHS) theory, that has its roots in the theory of Wertheim [22], as the soft-SAFT equation of state (EoS) used in this work, and that incorporates in its development the same structural idea. The authors used the BHS theory to account for repulsive interactions and the van der Waals one-fluid theory to describe attractive interactions. They found this approach accurate enough to describe properly the critical properties of alkanes, perfluoroalkanes and their mixtures. They observed that to correctly describe the UCST of the alkane + perfluoroalkanes mixtures, the correction parameter ξ in the geometric-mean rule for the van der Waals cross-term must be equal to 0.909 for all the mixtures studied. By applying this correction, they usually found that the difference between calculated and experimental values would not exceed 7%.

Recently, renewed interest on the subject came out with the work of McCabe et al. [23] and Colina et al. [24], both modelling the solution thermodynamics of alkane + perfluoroalkanes mixtures using the statistical associating fluid SAFT-VR approach. Interestingly, these authors found that to reproduce the observed mixing behaviour within the SAFT-VR model, the interaction energies between perfluoroalkane and alkane interaction sites had to be reduced by ca. 8% relative to the geometric-mean prediction, a result which is similar to that found by Knobler and co-workers. McCabe et al. [23] studied the high-pressure phase behaviour of a number of perfluro-*n*-alkane (C_1–C_4) + *n*-alkane

(C_1–C_7) binary mixtures, and suggested a value $\xi = 0.9234$. Later, Colina et al. [24] slightly modified this value to $\xi = 0.929$ in order to provide a better fit to the upper critical solution temperature (UCST) of the $C_6F_{14} + C_6H_{14}$ system. The unlike parameter was then used in a transferable way to predict liquid–liquid envelopes and the vapour–liquid phase behaviour of some of the mixtures measured by Lepori et al. [1]. As presented, the model could describe quite well the UCST of the mixtures but predicted narrower phase envelopes than the experimental ones. Also, the *P*–*x*–*y* diagrams were broader than those inferred from experimental data as a result of the overestimation of the pure component vapour pressures. In turn, the latter was due to a rescaling of the parameters to match the critical point, which made the predictions for subcritical properties less accurate.

Trying to overcome the higher deviations that McCabe et al. [23] observed when the chain length of the *n*-alkane component increased, Morgado et al. [2], also using the SAFT-VR EoS, concentrated on the behaviour of alkane + perfluoroalkane binary mixtures with chain lengths between five and eight carbon atoms for both components. They determined a set of binary interaction parameters that can be used to accurately predict the phase behaviour of alkane + perfluoroalkane systems of longer chain molecules and focused on the liquid–liquid immiscibility found close to ambient temperatures, rather than the high-pressure phase behaviour.

Song et al. [25] examined the use of typical all atom Lennard–Jones 12-6 plus Coulomb potential functions for simulating the interactions between perfluorinated molecules and alkanes together with the Lorentz–Berthelot combining rules usually employed with such potentials. This model had already been applied to accurately account for many of the liquid-phase properties of pure perfluoroalkanes [26] and alkanes [27], and the authors believed that departures from the geometric-mean rule mentioned above possibly resulted from inadequate treatment of molecular geometries or from charge distributions in the models employed in these earlier studies. However, they noticed that the special character of perfluoroalkane + alkane interactions was definitely not captured if standard combining rules were used. The authors compared their calculations with experimental data for second virial coefficients, gas–liquid solubilities and enthalpies of liquid mixing and observed that a reduction of ca. 10% in the interactions between unlike pairs of molecules was required, which is the same reduction required when simple single-site representations of molecules are used. Alternatively, the authors tried the use of two-parameter combining rules as well as more sophisticated approaches to calculate the cross-interaction parameters but the results were not conclusive. Ultimately, the underlying physical origins of the unusual mixing behaviour remained unclear.

In a recent work, Zhang and Siepmann [28] presented phase diagrams for selected *n*-alkanes, *n*-perfluoroalkanes and carbon dioxide ternary mixtures, as a function of pressure, from Monte Carlo simulations. They used two binary interaction parameters for the alkane–perfluoroalkane mixtures, fitted to a particular mixture, and used them in a transferable manner for the rest of the mixtures involving the two compounds. The agreement with the available data for the binary phase diagrams is fair, and hence a qualitative agreement with the ternary mixtures is expected.

In a previous study [29], our group used the soft-SAFT equation of state to model the experimental vapour–liquid equilibrium (VLE) and liquid–liquid equilibrium (LLE) data for PFCs + HCs measured by Lepori et al. [1]. The unlike energy parameter was treated as adjustable, and it was set at the optimum value $\xi = 0.9146$ for the correct prediction of the experimental azeotrope of the perfluoro-*n*-hexane + *n*-hexane mixture at 298.15 K. The unlike size parameter was not adjusted ($\eta = 1$), because the simple Lorentz combination rule provided satisfactory results. It is interesting to notice that the value of the unlike energy parameter agrees well with the values found by other authors using different models to describe these systems.

In this work, we present new data at both atmospheric pressure and high pressures for the LLE of perfluoro-*n*-octane with alkanes ranging from *n*-hexane to *n*-nonane. The experimental data measured is correlated using relations derived from renormalization group (RG) theory and Modified UNIFAC model with temperature dependent interaction parameters. Data are also modelled using the soft-SAFT equation of state in a predictive way by using the energetic interaction parameter obtained in our previous work [29] in a transferable manner. It is also shown that, to correctly describe the pressure dependence of the LLE data with the soft-SAFT EoS, both size and energy binary interaction parameters have to be considered.

2. Experimental

Liquid–liquid equilibria of binary mixtures of perfluoro-*n*-octane + alkanes, *n*-C_nH_{2n+2} ($n = 6$–9), were measured using synthetic methods: by turbidimetry at atmospheric pressure, and using laser light scattering techniques for measurements at pressures up to 150 MPa. All chemicals, from Aldrich, with claimed purities of 98% (perfluoro-*n*-octane) and 99% (alkanes) underwent further drying using 3 Å molecular sieves except the perfluoro-*n*-octane, which was used as received. Binary mixtures were gravimetrically prepared with an estimated weight fraction uncertainty of $\pm 2 \times 10^{-5}$.

In the case of measurements at a nominal pressure of 0.1 MPa, different samples of perfluoro-*n*-octane + *n*-alkane were prepared in ampoules containing a magnetic stirrer. Due to the density difference between the components, the heavier bottom phase is richer in PFC, and the upper phase contains mostly the hydrogenated component. The ampoules were sealed while frozen using liquid nitrogen to avoid changes in the composition of the samples. The ampoules containing mixtures at different compositions were then immersed in a thermostatic bath equipped with a calibrated Pt100 temperature sensor with an uncertainty of 0.05 K. Cloud points were determined by visual observation while heating the samples until a homogeneous phase is obtained followed by slow cooling of the mixtures until phase separation is detected.

Pressure effects on the liquid–liquid equilibrium temperature were obtained by He–Ne laser light scattering techniques using two apparatus. One of them, which operates up to pressures

of 5 MPa, has a thick-walled Pyrex glass tube cell (internal volume ~1.0 cm^3, optical length ~2.6 mm) connected to a pressurization line and separated from it by a mercury plug. The apparatus is easy, fast and safe to operate since both temperature and pressure are computer controlled and it is fully automated (including data acquisition and treatment). The apparatus, as well as the methodology used for the determination of phase transitions, have been recently described in detail [30]. Here, only a brief description is provided. Scattered light intensity is captured at a very low angle ($2^\circ < 2\theta < 4^\circ$) in the outer part of a bifurcated optical cable, while transmitted light is captured in the inner portion of this cable. The cloud point is the point on the $(I_{sc,corr})^{-1}$ against pressure (p) or temperature (T) least-squares fits where the slope changes abruptly. Temperature accuracy is typically ±0.01 K in the range 240 K < T < 400 K. As for pressure, accuracy is ±0.01 MPa up to 5 MPa. The other apparatus uses a stainless-steel cylindrical cell [31] closed on both sides with thick sapphire windows. It was used for experiments in which pressure was raised up to 150 MPa. In this case, the hydraulic fluid is the pure alkane in contact with a sufficiently long (1/16) in. stainless-steel tube filled with the solution (buffer volume), in order to avoid contamination during compression/expansion cycles. The total volume (buffer + optical) of injected solution is typically 1.6 cm^3, although the optical volume roughly corresponds to a mere 0.5 cm^3. In the case of isothermal runs, temperature accuracy is maintained (±0.01 K) but it worsens a bit for isobaric runs. As for pressure, the uncertainty is ±0.1 MPa in this higher-pressure range. Either cell can be operated in the isobaric or isothermal mode. Abrupt changes in either the transmitted or scattered light upon phase transition sharpen as the thermodynamic path approaches a perpendicular angle to the one-phase/two-phase surface. Pressure can be changed much more quickly than temperature, but, nonetheless, some experimental runs had to be performed in the isobaric mode due to the relatively low critical T–p slope presented by the current binary mixtures.

3. Modelling

3.1. Critical point estimation and data correlation

Systems with liquid–liquid equilibria present long-range concentration fluctuations in the vicinity of their consolute critical temperature. Asymptotically close to the critical point the thermodynamic properties vary as a simple power of the temperature difference or concentration difference (referred to their critical point values) with universal critical exponents, apart from a regular classical part. The non-classical behaviour of these systems as they approach their critical point is correctly taken into account from the renormalization group theory [32]. Since our liquid–liquid equilibria measurements are very close to the critical consolute temperature, we have correlated our experimental data using relations derived from the RG theory. According to Sengers et al. [33] the following relation is verified in the close vicinity of the critical point,

$$\Delta M = B(\tau)^{\beta} \quad (1)$$

where ΔM is the difference in the order parameter between the coexisting phases, β the exponent, B the amplitude, and $\tau = (T - T_c)/T_c$ holds for the reduced temperature that expresses the distance from the critical point. The order parameter is a quantity (mole fraction, volume fraction, density, etc.) chosen to measure the difference between the two coexisting phases. In the non-asymptotic region Eq. (1) is modified by the presence of corrections to scaling [34],

$$\Delta M = B_0\tau^{\beta}[1 + B_1\tau^{\Delta_1} + B_2\tau^{2\Delta_1} + \cdots] \quad (2)$$

where Δ_1 is the correction exponent. The so-called diameter of the coexisting curve is given by the relationship [35]

$$\frac{M_1^{I} + M_1^{II}}{2} = M_c[1 + A_1\tau + A_2\tau^{1-\alpha} + \cdots] \quad (3)$$

where α is a critical exponent and $M_1^{I} + M_1^{II}$, and M_c represent the property chosen for order parameter of component 1 in phases I, II, and at the critical point, respectively. When Eqs. (2) and (3) are combined (and perturbation terms are neglected) the result is the equation used in this work to correlate the experimental data:

$$\phi - \phi_c = fA\left(\frac{T - T_c}{T_c}\right)^{\beta} \quad (4)$$

where $f = 1$ for $x > x_c$ and $f = -1$ for $x < x_c$.

3.2. Modified UNIFAC model

Low pressure liquid–liquid equilibrium data are frequently modelled using an excess Gibbs energy model. The Modified UNIFAC model [36] was also used in this work to correlate the experimental data. The parameters required for the use of UNIFAC are group volumes (R_k), group surface areas (Q_k) and group-interaction parameters (a_{mn} and a_{nm}). The volume and area parameters for the groups involved in the mixtures studied (CF_2, CF_3, CH_2 and CH_3) are already available in the UNIFAC parameter table [37]. The group interaction parameters between the two main groups CF_2 and CH_2 have also been published for VLE predictions [37]. However, as discussed by Magnussen et al. [38], it is not possible to quantitatively predict LLE compositions using model parameters based on VLE data. In order to obtain a reliable prediction of multicomponent LLE using excess Gibbs energy models, it is necessary to establish the model parameters based on binary and ternary LLE data. In their work, the authors presented a set of interaction parameters adjusted to LLE data but that did not include the CF_2/CH_2 interaction. These interaction parameters were adjusted in this work using the experimental data measured.

The temperature dependence of the interaction parameters is described by the equation:

$$a_{mn} = a_{mn,1} + a_{mn,2}(T - T_0) \quad (5)$$

with $a_{mn} \neq a_{nm}$ and where T_0 is an arbitrary reference temperature, chosen to be 298.15 K in this work. The adjusted parameters $a_{mn,1}$ and $a_{mn,2}$ are equal to 146 and −0.3914 for the CF_2/CH_2 interaction and −7.66 and 0.2237 for the CH_2/CF_2 interaction.

The parameters were adjusted discarding the experimental data near the critical region giving a higher priority to the description of the diagrams far from that region.

3.3. The soft-SAFT EoS

We have also used a molecular-based EoS to describe the experimental data. The model was already used to study the vapour–liquid and liquid–liquid equilibrium data for PFCs + HCs mixtures [29]. More details about the model for these particular systems can be found in that work and in references therein. In this work, only the main equation is presented for completeness.

As usually done in SAFT-type equations, the soft-SAFT EoS is formulated in terms of the residual molar Helmholtz energy, A^{res}, defined as the molar Helmholtz energy of the fluid relative to that of an ideal gas at the same temperature and density. A^{res} is written as the sum of three contributions:

$$A^{res} = A^{total} - A^{ideal} = A^{ref} + A^{chain} + A^{assoc} \quad (6)$$

where A^{ref} accounts for the pairwise intermolecular interactions of the reference system, A^{chain} evaluates the free energy due to the formation of a chain from units of the reference system, and A^{assoc} takes into account the contribution due to site–site association. For molecules that do not associate, as those that are being studied in this work, the association term is null.

The SAFT model describes a pure non-associating fluid as homonuclear chains composed of equal spherical segments bonded tangentially. Different fluids will have different number of segments, m, segment diameter, σ, and segment interaction energy, ε. These parameters are usually obtained by adjusting the equation to density and vapour pressure data of the pure compounds. The molecular parameters for the compounds studied in this work had already been obtained and previously reported for perfluoro-*n*-octane [29] and for the linear alkanes from C_6 to C_9 [39]. When dealing with mixtures that are highly non-ideal, the Lorentz–Berthelot cross-interaction size and energy parameters need also to be adjusted to experimental data:

$$\sigma_{ij} = \eta_{ij}\frac{\sigma_{ii} + \sigma_{ij}}{2}, \quad (7)$$

$$\varepsilon_{ij} = \xi_{ij}\sqrt{\varepsilon_{ii}\varepsilon_{jj}} \quad (8)$$

The soft-SAFT equation has been accurately applied by our group to model VLE data for pure perfluoroalkanes [40], solubility data of gases as oxygen [29,41] and carbon dioxide [42] in these compounds and also VLE data for alkane and perfluoroalkanes systems [29]. In this last case, we have obtained that a single, temperature independent, energy binary parameter ($\xi_{ij} = 0.9146$), fitted to VLE equilibria for the system perfluoro-*n*-hexane + *n*-hexane mixture at 298.15 K is able to accurately describe the behaviour of this and other PFC–HC mixtures in a transferable manner [29]. We have further investigated the reliability of these parameters for describing the behaviour of other mixtures of PFC + HCs. Fig. 1 depicts experimental data for the $C_6H_{14} + C_7F_{16}$ mixture at 317.65 K and for the $C_6H_{14} + C_8F_{18}$ mixture at 313.15 K, both taken from ref. [43], as compared with soft-SAFT predictions using parameters from reference [29]. The predictive capability of these parameters is further shown in Fig. 2, where we show *P*–*x* diagrams at 259.95, 253.62, 246.35

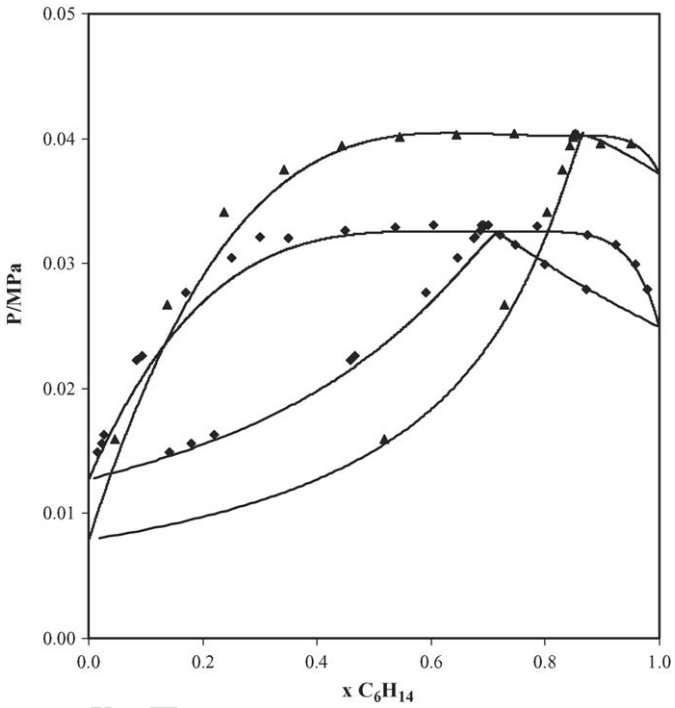

Fig. 1. *P*–*x*–*y* diagrams for $C_6H_{14} + C_7F_{16}$ at 317.65 K (diamonds) and $C_6H_{14} + C_8F_{18}$ at 313.15 K (triangles). Symbols represent experimental data by Duce et al. [43] and lines correspond to the predictions from the soft-SAFT EoS.

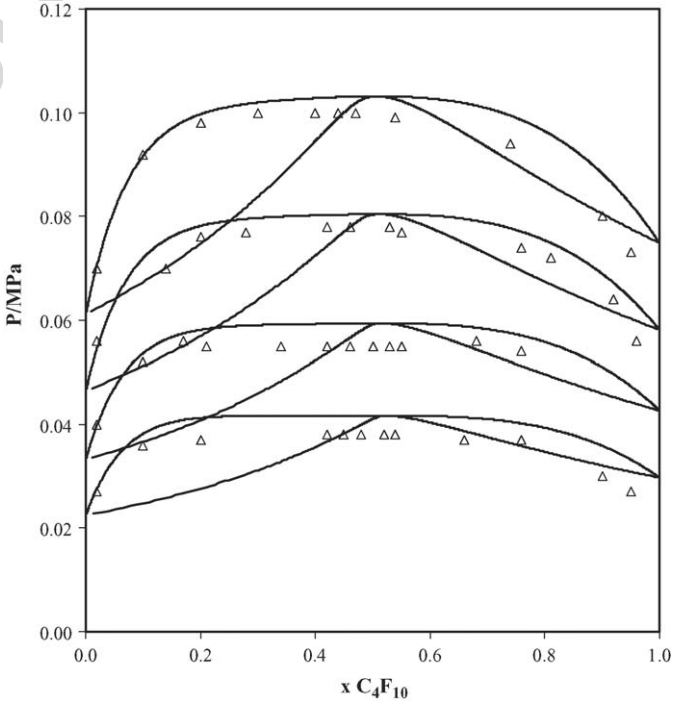

Fig. 2. *P*–*x*–*y* diagrams at 259.95, 253.62, 246.35 and 238.45 K for $C_4F_{10} + C_4H_{10}$ mixture compared with soft-SAFT predictions. The triangles describe the experimental data [44] and the solid curves the theoretical predictions as obtained by soft-SAFT.

and 238.45 K for $C_4F_{10} + C_4H_{10}$ mixture [44] compared with soft-SAFT predictions. The excellent agreement found between the experimental data and the soft-SAFT predictions in all these cases has encouraged the use of an identical set of parameters for the LLE data measured in this work, in order to further check their transferability for other regions of the phase diagram.

4. Results and discussion

Experimental data measured for the studied systems at atmospheric pressure and high pressure are reported in Tables 2 and 3, respectively. Experimental data at a nominal pressure of 0.1 MPa are presented in Fig. 3a and b where compositions are expressed in terms of mole and volume fraction, respectively. Compositions in terms of volume fractions (ϕ) are calculated using the relation:

$$\phi_i = \frac{x_i}{x_i + K(1 - x_i)} \quad (9)$$

where $K = \rho_i M_j / \rho_j M_i$, being ρ and M the mass density and the molecular weight, respectively, of components i and j. As for most systems, it occurs that the temperature versus composition diagrams of PFCs + HCs mixtures are more symmetric when represented in terms of volume fraction as compared to mole fraction.

Fig. 3a also compares the data measured in this work with the experimental data recently published by Lo Nostro et al. [3]. It can be observed that the results agree well for the perfluoro-*n*-octane + *n*-octane mixture but significant deviations are observed for perfluoro-*n*-octane with *n*-hexane and especially with *n*-heptane. The higher deviations found in mixtures involving volatile compounds, as is the case of *n*-hexane and *n*-heptane, may be justified by changes in the composition of the mixtures during the measurement procedure.

As mentioned in the previous section our experimental data were correlated using relations derived from renormalization group theory, in which the volume fraction was chosen to be the order parameter. Eq. (4) was used to correlate our mutual solubility experimental data in the entire temperature interval, including the critical region. Values for A and β to be used in Eq. (4) together with the calculated values for the critical temperature, mole fraction, and volume fraction for each mixture are reported in Table 4. The solid lines in Fig. 3a and b represent the correlations.

Table 2
Experimental liquid–liquid solubility data for perfluoro-*n*-octane (1) + alkane (2) (C_6–C_9) mixtures at atmospheric pressure

$C_8F_{18} + C_6H_{14}$		$C_8F_{18} + C_7H_{16}$		$C_8F_{18} + C_8H_{18}$		$C_8F_{18} + C_9H_{20}$	
T (K)	x_1	T (K)	x_1	T (K)	x_1	T (K)	x_1
293.98	0.0806	319.13	0.1024	334.24	0.0991	352.09	0.1116
306.36	0.1222	328.21	0.1772	345.48	0.1669	362.24	0.1650
308.95	0.1683	330.76	0.2611	349.16	0.2374	367.65	0.2526
310.83	0.2518	330.76	0.3185	350.52	0.3013	368.85	0.3505
310.81	0.2997	330.96	0.3818	350.44	0.4026	368.49	0.4342
310.71	0.3470	330.58	0.4967	349.70	0.4984	367.46	0.5395
310.65	0.3959	329.80	0.5437	346.09	0.5964	362.59	0.6391
309.61	0.4425	316.24	0.7048	336.01	0.7245	349.16	0.7639
308.49	0.4891			327.71	0.7640	322.99	0.8805
305.74	0.5440			299.71	0.8919		
303.05	0.6000						
296.93	0.6657						
293.89	0.6924						

Table 3
Experimental liquid–liquid solubility data for perfluoro-*n*-octane (1) + alkane (2) (C_6–C_9) mixtures at pressures higher than atmospheric

$C_8F_{18} + C_6H_{14}$

$x_1 = 0.2552$		$x_1 = 0.2678$		$x_1 = 0.2644$	
T/K	P/MPa	T/K	P/MPa	T/K	P/MPa
311.58	1.48	311.13	0.85	311.72	1.43
312.08	2.18	311.80	1.74	312.52	2.45
312.59	2.88	311.41	1.23	313.29	3.40
313.31	3.78	310.89	0.53	314.02	4.42
314.12	4.95	313.24	3.60	314.81	5.45
310.98	0.71	312.42	2.57	322.99	16.70
310.53	0.13			332.97	31.00
				342.95	46.50
				353.00	62.80
				363.07	80.20
				373.16	98.00
				383.43	118.50
				394.15	143.00

$C_8F_{18} + C_7H_{16}$

$x_1 = 0.2567$		$x_1 = 0.3446$	
T/K	P/MPa	T/K	P/MPa
331.90	1.52	330.88	0.14
333.29	3.20	331.33	0.60
333.78	3.83	331.92	1.37
332.48	2.24	332.82	2.41
		333.50	3.28
		334.49	4.46

$C_8F_{18} + C_8H_{18}$

$x_1 = 0.3608$		$x_1 = 0.7510$	
T/K	P/MPa	T/K	P/MPa
349.80	0.15	332.302	4.02
350.18	0.60	331.999	3.55
350.93	1.48	331.619	3.04
351.80	2.49	331.124	2.54
352.64	3.46	330.628	1.87
353.44	4.42	332.604	4.26
		329.668	0.70
		329.308	0.29
		330.127	1.27

$C_8F_{18} + C_9H_{20}$

$x_1 = 0.0828$	
T/K	P/MPa
344.34	0.16
344.68	0.84
345.34	1.85
345.78	2.50
346.46	3.48
347.12	4.41

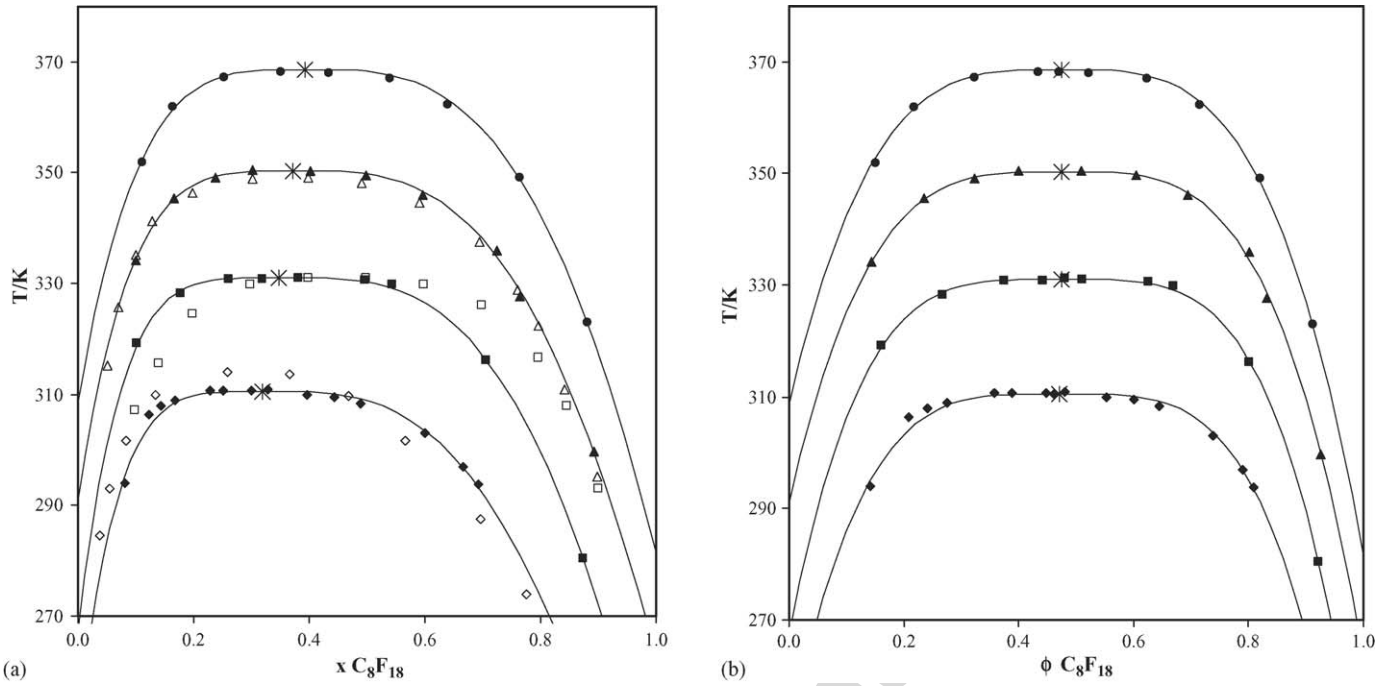

Fig. 3. Experimental and correlated coexisting curve of perfluoro-*n*-octane + alkanes (C_6–C_9) in terms of mole fraction (a) and volume fraction (b). Symbols represent solubility in *n*-hexane (♦), *n*-heptane (■), *n*-octane (▲) and *n*-nonane (●). (✳) Represents the critical point for each mixture. The non-filled symbols in Fig. 1a represent data measured by Lo Nostro et al. [3]. The lines represent the correlated data calculated from renormalization group theory.

Fig. 4 shows a comparison between the experimental LLE data for $C_8F_{18} + C_nH_{2n+2}$ at 1MPa and two models: the modified UNIFAC model (dashed lines) and the soft-SAFT EoS (solid lines). Note that the UNIFAC model has been fitted to the binary data using four adjustable parameters, while results from soft-SAFT are pure predictions since the parameters used were obtained from fitting VLE data. Even though the agreement of soft-SAFT with the experimental data is not as accurate at that shown in Figs. 1 and 2, the EoS provides an acceptable description of the experimental data in the region far from the critical point and even the trend of the critical point shift with the alkane chain length change in the mixture is well captured. Since most classical models are not accurate in describing LLE and, in addition, no fitting to these data has been performed, those should be considered as good predictions. Also, notice that no long-range fluctuations are included in the version of soft-SAFT used here, and hence, a correct description of the critical region should not be expected. An alternative approach would be to use the crossover-soft-SAFT EoS [45,46], which correctly describes both the regions far from and close to the VLE critical point of pure fluids and binary mixtures. However, two reasons have prevented us from using the crossover equation

Table 4
Parameters to be used in Eq. (4) together with critical constants for the studied mixtures

System	A	β	ϕ_c	x_c	T_c
$C_8F_{18} + C_6H_{14}$	0.71426	0.25801	0.471	0.320	310.54
$C_8F_{18} + C_7H_{16}$	0.71572	0.25017	0.474	0.348	330.99
$C_8F_{18} + C_8H_{18}$	0.77238	0.27603	0.473	0.371	350.33
$C_8F_{18} + C_9H_{20}$	0.79521	0.28589	0.473	0.393	368.65

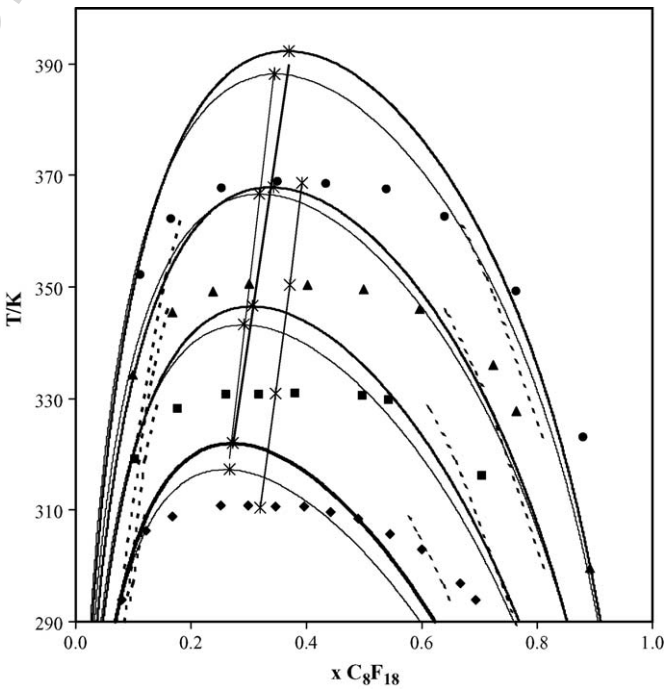

Fig. 4. Comparison between experimental LLE data for $C_8F_{18} + C_nH_{2n+2}$ mixtures at 0.1 MPa and the predictions obtained from the soft-SAFT EoS. Symbols represent the experimental data as in Fig. 1. The full lines represent the predictions given by the soft-SAFT EoS when $\eta = 1$ and $\xi = 0.9146$ (▬) and $\eta = 1.011$ and $\xi = 0.9146$ (—) and the dashed lines the correlation results obtained with the Modified UNIFAC model. Stars represent the upper critical solution temperature for each mixture.

in this work: first of all, our purpose here was to check the transferability of the parameters obtained from other regions of the phase diagram of these mixtures and of related ones (which were fitted with the classical soft-SAFT EoS), and secondly, as discussed in ref. [46], the crossover-soft-SAFT equation is not ready, yet, for LLE, since the isomorphism assumption used to develop it does not apply to this type of phase equilibria.

The soft-SAFT model has also been used to predict the pressure dependence of the phase diagrams. In this case, the size binary interaction parameter had to be slightly adjusted to a value equal to 1.011 in order to correctly describe the pressure dependence of the experimental data. This change is related with the excess volume description of the mixtures by the soft-SAFT model and has little influence on the description of the LLE data at atmospheric pressure as shown in Fig. 4. It is interesting to observe that the size and energy binary interaction parameters used in this work are very similar to the adjusted unlike CH_x/CF_y cross-interaction parameters used by Zhang and Siepmann [28] when using molecular simulation to model alkane + perfluoroalkane mixtures.

The results given by the model to describe the high-pressure data are compared with the experimental results in Fig. 5 for the $C_8F_{18} + C_6H_{14}$ mixture at $x = 0.2644$. Table 5 compares the experimental and calculated $(\partial T/\partial P)_x$ for distinct fixed compositions of all the mixtures studied. Although the model overpredictes the experimental temperature, as expected because there was not a perfect match at atmospheric pressure, the pressure dependence is correctly predicted. A comparison between the predictive results obtained with the soft-SAFT and the correlated data obtained with the Modified UNIFAC model, using

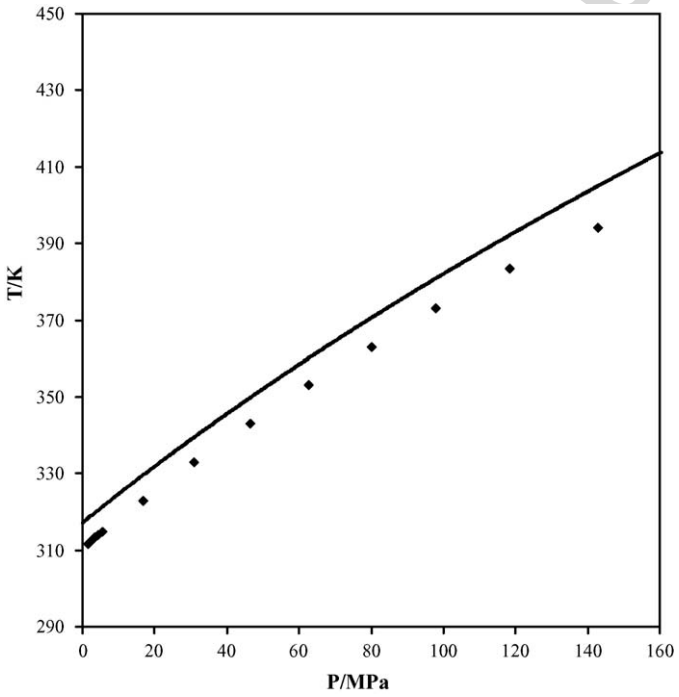

Fig. 5. Effect of the pressure on the LLE of $C_8F_{18} + C_6H_{14}$ mixtures at $x_{C8F18} = 0.2644$. The line represents the predictions given by the soft-SAFT EoS when $\eta = 1.011$ and $\xi = 0.9146$.

Table 5
Experimental and calculated $(\partial T/\partial P)_x$ for distinct fixed compositions of all the mixtures studied

System	x_{C8F18}	$(\partial T/\partial P)_x$ (K bar^{-1})	
		Experimental ($\times 10^2$)	Calculated ($\times 10^2$)
$C_8F_{18} + C_6H_{14}$	0.2552	7.47	7.51
	0.2678	7.63	7.56
$C_8F_{18} + C_7H_{16}$	0.2567	8.18	7.70
	0.3446	8.29	8.20
$C_8F_{18} + C_8H_{18}$	0.3608	8.54	8.37
	0.7510	8.17	7.73
$C_8F_{18} + C_9H_{20}$	0.0828	6.61	5.04

interaction parameters explicitly adjusted to describe LLE data, let us conclude that the predictive capacity of the soft-SAFT model is superior.

In the case of one of the systems studied, $C_8F_{18} + C_6H_{14}$, it is possible to estimate the magnitude of the molar excess enthalpy, a quantity that has seldom been investigated in these systems. Under some restrictive assumptions [47], the Prigogine–Defay equation establishes a Clapeyron-type of relationship in which the pressure dependence of the critical temperature is directly related to the excess properties themselves:

$$\left(\frac{\mathrm{d}T}{\mathrm{d}p}\right)_c \cong T_c \frac{v^E(T_c(p), x)}{h^E(T_c(p), x)} \tag{10}$$

Recently, Rebelo et al. [48] demonstrated that Eq. (10) can also be successfully applied at temperatures and finite concentrations not too far from critical. At 298.15 K, the $C_8F_{18} + C_6H_{14}$ system is heterogeneous for the equimolar composition. Nonetheless, by Redlich–Kister interpolation it is possible to determine the hypothetical, equimolar reference value for any excess property provided there are sufficient data in the homogeneous region. This was done by Lepori et al. [1] who reported a value of 5.1 cm^3 mol^{-1} for the equimolar excess volume at 298.15 K. The use of the Prigogine and Defay relation (Eq. (10)) thus establishes 2.03 kJ mol^{-1} for the endothermic equimolar excess enthalpy at 298.15 K to be compared with the experimental values 2.16 and 2.37 kJ mol^{-1} [49,50] for the similar $C_6F_{14} + C_6H_{14}$ system.

5. Conclusions

In this work, we have presented liquid–liquid equilibrium of binary mixtures of perfluoro-*n*-octane + alkanes, *n*-C_nH_{2n+2} ($n = 6$–9), as measured by turbidimetry at atmospheric pressure, and using a laser light scattering technique for measurements at pressures up to 150 MPa. A group renormalization theory was used to calculate the critical temperature and mole fraction for each mixture, which are difficult to observe experimentally due to the extended flatness region that these systems exhibit. The Modified UNIFAC model was used to correlate the experimental data using interaction parameters that are temperature dependent. Results obtained from the correlation were compared with the predictive results obtained with the soft-SAFT model using

interactions parameters adjusted to VLE data. The comparison showed that the results obtained with the soft-SAFT model are of better quality than those correlated by UNIFAC, corroborating the higher predictive capacity of the soft-SAFT model.

List of symbols

a_{mn}	UNIFAC group-interaction parameters
A	Helmholtz free energy
h^{E}	excess enthalpy
m	chain length (for Lennard–Jones segments)
M	molecular weight
ΔM	difference in the order parameter between the coexisting phases
P	pressure
Q_{k}	UNIFAC group surface areas
R_{k}	UNIFAC group volumes
T	temperature
T_0	reference temperature equal to 298.15 K
v^{E}	excess volume
x	mole fraction

Greek letters

α	critical exponent
β	critical exponent
Δ_1	correction exponent
ε	segment interaction energy (between Lennard–Jones segments)
η	size parameter of the generalized Lorentz–Berthelot combination rules
ξ	energy parameter of the generalized Lorentz–Berthelot combination rules
ρ	mass density (kg/m^3)
σ	size parameter of the intermolecular potential/diameter (for Lennard–Jones segments)
τ	reduced temperature that expresses the distance from the critical point
ϕ	volume fraction

Indices

assoc	association term for soft-SAFT EoS
c	critical
Chain	chain term for soft-SAFT EoS
i	component
ref	reference term for soft-SAFT EoS
I	phase one
II	phase two

Acknowledgements

Several helpful discussions with Fèlix Llovell (Institut de Ciència de Materials de Barcelona, Barcelona, Spain) are gratefully acknowledged. This project was financed by Fundação para a Ciência e Tecnologia, POCTI/35435/EQU/2000. A.M.A. Dias is grateful to Fundação para a Ciência e Tecnologia for the Ph.D. grant SFRH/BD/5390/2001. Partial support has been provided by the Spanish government, under projects HP2002-0089, CTQ2004-05985-C02-01 and CTQ2005-00296/PPQ.

References

[1] L. Lepori, E. Matteoli, A. Spanedda, C. Ducè, M.R. Tine, Fluid Phase Equilib. 201 (2002) 119–134.
[2] P. Morgado, C. McCabe, E.J.M. Filipe, Fluid Phase Equilib. 228–229 (2005) 389–393.
[3] P. Lo Nostro, L. Scalise, P. Baglioni, J. Chem. Eng. Data 50 (2005) 1148–1152.
[4] I.A. McLure, R. Whitfield, J. Bowers, J. Colloid Interface Sci. 203 (1998) 31–40.
[5] I.T. Horvath, J. Rabai, Science 266 (1994) 72–75.
[6] A. Studer, S. Hadida, R. Ferritto, S.Y. Kim, P. Jeger, P. Wipf, D.P. Curran, Science 275 (1997) 823–826.
[7] B. Betzemeier, P. Knochel, Top. Curr. Chem. 206 (1999) 61–78.
[8] J.H. Hildebrand, D.R.F. Cochran, J. Am. Chem. Soc. 71 (1949) 22–25.
[9] J.H. Hildebrand, B.B. Fisher, H.A. Benesi, J. Am. Chem. Soc. 72 (1950) 4348–4351.
[10] J.H. Simons, R.D. Dunlap, J. Chem. Phys. 18 (1950) 335–346.
[11] J.H. Simons, J.W. Mausteller, J. Chem. Phys. 20 (1952) 1516–1519.
[12] D.N. Campbell, J.B. Hickman, J. Am. Chem. Soc. 75 (1953) 2879–2881.
[13] J.B. Hickman, J. Am. Chem. Soc. 77 (1955) 6154–6156.
[14] R.G. Bedford, R.D. Dunlap, J. Am. Chem. Soc. 80 (1958) 282–285.
[15] J.H. Hildebrand, R.L. Scott, Solubility of Nonelectrolytes, third ed., Reinhold Publishing Corp., New York, 1950.
[16] R.L. Scott, J. Phys. Chem. 62 (1958) 136–145.
[17] E.M.D. Siebert, C.M. Knobler, J. Phys. Chem. 75 (1971) 3863–3870.
[18] D.E.L. Dyke, J.S. Rowlinson, R. Thacker, Trans. Faraday Soc. 55 (1959) 903–910.
[19] J.S. Rowlinson, Liquids and Liquid Mixtures, second ed., Butterworth Scientific, London, 1969.
[20] A.E.H.N. Mousa, A. Kreglews, W.B. Kay, J. Chem. Thermodyn. 4 (1972) 301–305.
[21] A.L. Archer, M.D. Amos, G. Jackson, I.A. McLure, Int. J. Thermophys. 17 (1966) 201–206.
[22] M.S. Wertheim, J. Stat. Phys. 35 (1984) 35–47.
[23] C. McCabe, A. Galindo, A. Gil-Villegas, G. Jackson, J. Phys. Chem. B 102 (1998) 8060–8069.
[24] C.M. Colina, A. Galindo, F.J. Blas, K.E. Gubbins, Fluid Phase Equilib. 222 (2004) 77–85.
[25] W. Song, P.J. Rossky, M. Maroncelli, J. Chem. Chem. Phys. 119 (2003) 9145–9162.
[26] E.K. Watkins, W.L. Jorgensen, J. Phys. Chem. A 105 (2001) 4118–4125.
[27] W.L. Jorgensen, D.S. Maxwell, J. Tirado-Rives, J. Am. Chem. Soc. 118 (1996) 11225–11236.
[28] L. Zhang, J.I. Siepmann, J. Phys. Chem. B 109 (2005) 2911–2919.
[29] A.M.A. Dias, J.C. Pàmies, J.A.P. Coutinho, I.M. Marrucho, L.F. Vega, J. Phys. Chem. B 108 (2004) 1450–1457.
[30] H.C. Sousa, L.P.N. Rebelo, J. Chem. Thermodyn. 32 (2000) 355–387.
[31] L.P.N. Rebelo, Z.P. Visak, H.C. Sousa, J. Szydlowski, R. Gomes de Azevedo, A.M. Ramos, V. Najdanovic-Visak, M. Nunes da Ponte, J. Klein, Macromolecules 35 (2002) 1887–1895.
[32] T. Narayanan, A. Kumar, E.S.R. Gopal, S.C. Greer, J. Phys. Chem. 84 (1980) 2883–2887.
[33] J.M.H.L. Sengers, W.L. Greer, J.V. Sengers, J. Phys. Chem. Ref. Data 5 (1976) 1–52.
[34] F.J. Wegner, Phys. Rev. B 5 (1972) 4529–4536.
[35] L. Koo, M.S. Green, Phys. Rev. A 16 (1977) 2483–2487.
[36] B.L. Larsen, P. Rasmussen, A. Fredenslund, Ind. Eng. Chem. Res. 26 (1987) 2274–2286.
[37] H.K. Hansen, P. Rasmussen, A. Fredenslund, M. Schiller, J. Gmehling, Ind. Eng. Chem. Res. 30 (1991) 2352–2355.
[38] T. Magnussen, P. Rasmussen, A. Fredenslund, Ind. Eng. Chem. Process Des. Dev. 20 (1981) 331–339.
[39] J.C. Pàmies, L.F. Vega, Ind. Eng. Chem. Res. 40 (2001) 2532–2543.
[40] A.M.A. Dias, C.M. Gonçalves, A.I. Caço, L.M.N.B.F. Santos, M.M. Piñeiro, L.F. Vega, J.A.P. Coutinho, I.M. Marrucho, J. Chem. Eng. Data 50 (2005) 1328–1333.

[41] A.M.A. Dias, J.C. Pamiés, L.F. Vega, J.A.P. Coutinho, I.M. Marrucho, J. Polish Chem. 80 (2006) 143–152.
[42] A.M.A. Dias, J.C. Pamiés, H. Carrier, J.L. Daridon, L.F. Vega, J.A.P. Coutinho, I.M. Marrucho, IECR (2006) in press.
[43] C. Duce, M. Tine, L. Lepori, E. Matteoli, Fluid Phase Equilib. 199 (2002) 197–212.
[44] J.A. Brown, W.H. Mears, J. Phys. Chem. 62 (1958) 960–962.
[45] F. Llovell, J.C. Pàmies, L.F. Vega, J. Chem. Phys. 121 (2004) 10715–10724.
[46] F. Llovell, L.F. Vega, J. Phys. Chem. 110 (2006) 1350–1362.
[47] L.P.N. Rebelo, Phys. Chem. Chem. Phys. 1 (1999) 4277–4286.
[48] L.P.N. Rebelo, V. Najdanovic-Visak, Z.P. Visak, M. Nunes da Ponte, J. Troncoso, C.A. Cerdeiriña, L. Romani, Phys. Chem. Chem. Phys. 4 (2002) 2251–2259.
[49] A.G. Williamson, R.L. Scott, J. Phys. Chem. 65 (1961) 275–279.
[50] R.D. Dunlap, R.G. Bedford, J.C. Woodbrey, S.D. Furrow, J. Am. Chem. Soc. 81 (1959) 2927–2930.